Semicond. Sci. Technol. 8 (1993) 922–927. Printed in the UK

Novel techniques for characterizing detector materials using pulsed infrared synchrotron radiation

G L Carr†, J Reichman†, D DiMarzio†, M B Lee†, D L Ederer‡, K E Miyano‡, D R Mueller§, A Vasilakis‖ and W L O'Brien¶*

† Grumman Corporate Research Center, Bethpage, NY 11714, USA
‡ Department of Physics, Tulane University, New Orleans, LA 70118, USA
§ National Institute of Standards and Technology, Gaithersburg, MD 20899, USA
‖ Physics Department, Long Island University-CW Post, Brookville, NY 11548, USA
¶ Physics Department, University of Tennessee, Knoxville, TN 37996, USA

Abstract. The VUV ring at the National Synchrotron Light Source (NSLS, Brookhaven National Laboratory) is a source of nanosecond-duration, high-brightness, broadband IR pulses. We are developing several measurement techniques for characterizing $Hg_{1-x}Cd_xTe$ and other IR detector materials using this source. For example, the broadband IR pulses can be used to study transient photoconductive decay at various photon energies near the bandgap. A particularly novel technique we have developed is far-infrared photoinduced nanosecond spectroscopy (FIR-PINS). In this all-optical (contactless) measurement, a short laser pulse generates photocarriers which are subsequently sensed by a far-infrared pulse from the synchrotron. Spectroscopic analysis of the far-infrared yields the free carrier plasma frequency, providing information on the photocarrier density. By varying the delay time of the far-infrared pulse (relative to the laser pulse), the photocarrier relaxation is determined with nanosecond resolution. In addition to being contactless, the technique offers other potential advantages over electrical measurements. Results for MBE-grown $Hg_{1-x}Cd_xTe$ are presented.

1. Introduction

1.1. Photocarrier lifetime studies

The process of photocarrier generation and relaxation is central to infrared detection in semiconductors. For this reason, the characterization of a detector material typically includes measurements of photocarrier decay. In the bulk, the lifetime is determined by the rates at which electrons and holes recombine via three processes: radiative, Auger and Shockley–Read. A fourth recombination process occurs at surface defects. A long lifetime is desired for detector applications requiring sensitivity rather than speed. The radiative and Auger recombination rates are determined by the carrier concentration and the band structure. For a given material, they impose intrinsic upper limits on the lifetime. Shockley–Read recombination occurs at defects, and can be the mechanism which limits the ultimate detector performance. Control of such defects is critical for producing high-performance detector material.

In general, all four recombination mechanisms play a role in $Hg_{1-x}Cd_xTe$ (MCT). Separating the contributions of each and relating them to material properties is a major goal of photoconductivity lifetime studies. Though the lifetime can be inferred from the equilibrium response to a continuous source of light, time-dependent measurements yield a more complete picture of the photocarrier decay process. This is particularly true when the decay is not a simple exponential with a unique time constant [1]. One common measurement technique is photoconductivity decay (PCD) [2], where a pulse of light generates carriers and their decay is monitored through the time dependence of the conductivity. When Shockley–Read recombination is dominant, a detailed PCD study provides information on the nature of the defect.

In typical PCD measurements, photocarriers are generated with a pulsed laser and the change in conductivity is sensed with an oscilloscope. Therefore electrical contacts must be attached to the sample's surface, a disruptive and potentially destructive process. Contactless techniques, using microwaves [3] or infrared [4, 5] sources to sense the carriers, have been developed to circumvent this problem. Microwaves are reasonably sensitive to changes in electrical conductivity, but lack

* Present address: Synchrotron Radiation Center, Stoughton, WI 53589, USA.

0268-1242/93/060922+06 $07.50

high spatial resolution. The sensitivity to direct absorption by free carriers at infrared wavelengths ($\lambda < 20$ μm) is low, so quantitative information on photocarrier densities is not readily obtained. The pulsed laser source that generates the carriers is often poorly matched to the photoconductive material. The photon energy may be far above the bandgap, for which the absorption coefficient is high, resulting in photocarrier generation within the first micrometre of material. The results can be overly sensitive to high surface recombination velocities, or variations in material properties with depth.

In this paper we describe two photoconductivity measurement techniques, based on the unique properties of infrared synchrotron radiation (IR-SR), that solve some of the problems described above. In particular, we show our initial results using IR-SR to produce photocarriers at varying depths into a film and also to sense their decay.

We evaluated these techniques using a 10 μm thick film of $Hg_{0.76}Cd_{0.24}Te$ grown on CdTe by molecular beam epitaxy (MBE). The sample was n type with a low-temperature (extrinsic) carrier concentration of 3×10^{15} cm^{-3}, as determined by Hall measurements. The surface was intentionally left untreated. Conventional PCD measurements revealed a lifetime of 20 ns or less.

1.2. Infrared synchrotron radiation

Synchrotron radiation is produced when electrons, travelling at relativistic speeds, pass through the strong magnetic fields needed to bend them around a closed orbit. The electrons travel in bunches, and each bunch produces a pulse of light when it passes through a bending magnet. There now exist dedicated facilities for producing synchrotron radiation, including the National Synchrotron Light Source (NSLS) at Brookhaven National Laboratory. Though the peak flux occurs in the x-ray region, the range of emitted wavelengths extends down into the microwave region.

The IR-SR source for this study was the NSLS beamline U4IR. The detailed characteristics of the source are described elsewhere [6]. We note here those features useful for studying IR materials. First, the output has continuous wavelength coverage to beyond 1000 μm. The source has very high brightness, but lower average power, when compared with a blackbody source (the exception being at very long wavelengths where the average power can exceed that of a blackbody source by a factor of 10 or more). Finally, the output is pulsed with a 1 ns duration. In the standard mode of operation, seven electron bunches orbit simultaneously, and the pulse separation is ~19 ns. In single-bunch operation, the pulse separation is the ring's orbital period of 170 ns.

2. Measurements

2.1. Wavelength-dependent photoconductivity decay

IR-SR can be used as a pulsed source for studying transient photoconductivity decay. The pulse structure is fairly well matched to the range of carrier lifetimes found in narrow-gap materials. The exceptionally broad spectral output covers a wide range of photoconductive materials. The U4IR beamline source has already proved useful in studying fast superconducting infrared bolometers [7].

Model calculations for surface recombination effects indicate that the transient photocarrier response depends on the absorption (penetration) depth δ for the light. This dependence could be used to distinguish surface from bulk recombination processes. The absorption coefficient for MCT varies strongly for photo energies near the bandgap. A photon source which could be tuned through the bandgap would provide the means to perform PCD measurements as a function of δ. The bandgap in MCT depends on the x value, spanning photon energies from below 50 meV to several hundred meV. Even for a given x value, the bandgap changes considerably with temperature. Pulsed laser sources provide a more than adequate photon flux, but the wavelength coverage is very limited. IR-SR has complete wavelength coverage, but the photon flux depends on the wavelength (or energy) bandwidth.

The generation of photocarriers in MCT is a quantum process in which each photon generates at most a single electron–hole pair. Therefore, the photon fluence is the important parameter for characterizing a source in PCD measurements. A survey of the absorption coefficient for a variety of MCT samples [8] shows that the penetration depth changes by one decade within a 10 meV photon energy band, near the bandgap. The U4IR (IR-SR) photon fluence for a 10 meV bandwidth can be readily calculated from the NSLS VUV ring's operating parameters. Assuming light collection optics that produce a 0.5 mm diameter spot on the sample, the photon fluence (per pulse) is 10^{10} photons/cm^2, or more, throughout the energy range of interest. With a penetration depth of 10 μm, photocarrier concentrations approaching 10^{13} cm^{-3} occur. This compares favourably with the equilibrium carrier concentrations for most materials, and should result in measurable signals.

For the actual measurements, short wires connected the MCT film sample to a 50 Ω coaxial cable. The electrical signals were amplified (10 kHz to 1.3 GHz bandwidth, 26 dB gain) and fed to a digitizing oscilloscope (DC to 1 GHz bandwidth). The sample was current biased at a few milliamperes, applied through the same coaxial cable with a bias tee. The sample resistance was between 200 Ω and 300 Ω, which gave less than ideal coupling to the 50 Ω cable, but would not result in serious waveform distortion.

The MCT sample was placed in a vacuum chamber connected to the beamline and cooled with an open-cycle helium refrigerator. The $f/10$ beam from the U4IR port was focused onto the sample with an ellipsoidal reflector, producing a 0.3 mm diameter spot. A set of three filters before the sample was used to select a particular wavelength band: $\lambda > 0.5$ μm (no filter), 3 μm $< \lambda <$ 5 μm and 7.5 μm $< \lambda <$ 12 μm. These are far wider than the 10 meV bandpass suggested above, but can give similar results when the bandgap and filter overlap slightly.

Photoresponse measurements were made with the

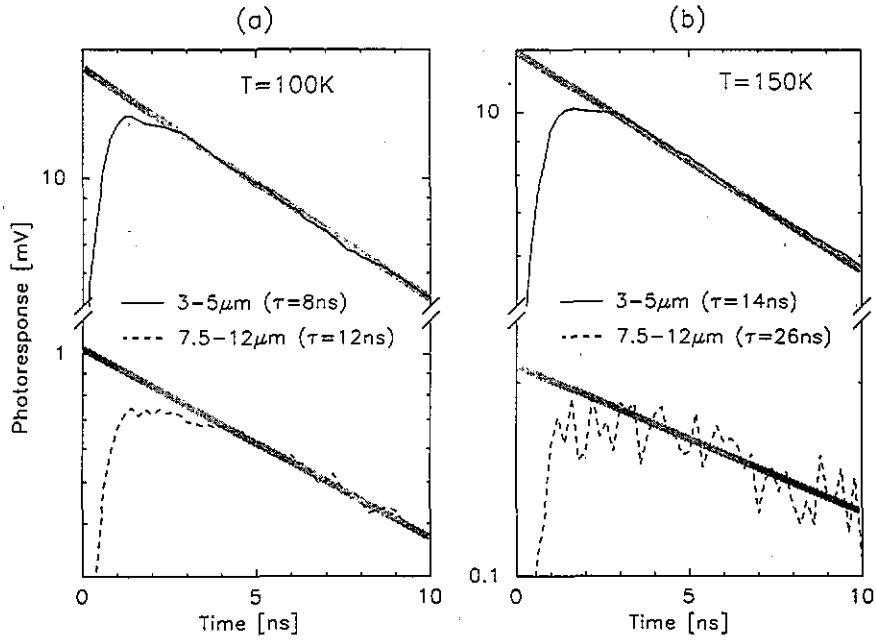

Figure 1. Photoresponse of MCT for two wavelength bands of incident photons (3 μm–5 μm and 7.5 μm–12 μm). The gray hatchings are guides to the eye only.

VUV ring operating in one-bunch mode. The signals were found to be linear in bias current and incident intensity with no evidence for spurious photovoltaic effects due to electrical contacts. To allow for direct comparisons, we normalized the data to the photon flux for a given filter. The results for the full band and the 3–5 μm band were consistent at all temperatures. In both of these cases the photocarriers are generated near the front surface. Above 200 K, the bandgap for $Hg_{0.76}Cd_{0.24}Te$ corresponds to wavelengths smaller than 7 μm, and no measurable signal was obtained for the 7.5–12 μm band, as expected. As the sample was cooled the bandgap shifted downward. By 150 K, weak absorption began at $\lambda = 7.5$ μm and a signal appeared. The penetration depth exceeded the film thickness, and photocarriers were produced more or less uniformly. The band edge continued to decrease with temperature, and the signal for the 7.5–12 μm band grew larger. For $T = 100$ K and lower, a substantial number of photons were absorbed near the front surface.

The photoresponse signals for two wavelength bands and two sample temperatures are shown in figure 1. The most striking difference is observed at $T = 150$ K, where the initial (first few nanoseconds) photocarrier recombination rate ($1/\tau$) for 7.5–12 μm photons is approximately 1/2 that for 3–5 μm photons. This illustrates the sensitivity of the photocarrier decay to the penetration depth and initial photocarrier distribution. We conclude that a high surface recombination velocity exists, leading to the short initial lifetime observed for the 3–5 μm photons.

2.2. Photoinduced nanosecond spectroscopy of $Hg_{1-x}Cd_xTe$ in the far-IR

In the preceding section we demonstrated the capability of IR-SR to produce photocarriers in a PCD measurement. However, electrical contacts were still required. In this section, we describe a particularly novel technique for sensing the photocarrier decay without contacts. To accomplish this, we will utilize the portion of the IR-SR beyond $\lambda = 100$ μm to sense the number of photocarriers.

The optical properties of a material can be conveniently described by a frequency-dependent complex conductivity (or dielectric function). In many materials, the contribution of free carriers to the optical conductivity is well described by a Drude function

$$\sigma(\omega) = \frac{\sigma_0}{1 - i\omega\tau}$$

where $\sigma_0 = ne^2\tau/m^*$ is the DC conductivity, and n, e, τ and m^* are the carrier concentration, charge per carrier, scattering time and effective mass respectively. Note that for frequencies $\omega \gg 1/\tau$, the conductivity approaches zero. The scattering time can be estimated from the mobility ($\mu = e\tau/m^*$) and effective mass. At low temperatures, values of $\mu \sim 10^4$ cm^2 V^{-1} s^{-1} and $m^* = 0.01m_0$ are typical, resulting in $\tau \sim 10^{-13}$ s. Therefore, the conductivity is appreciable only for $\omega \sim 1/\tau$ or smaller, corresponding to wavelengths beyond 100 μm (in the far-infrared).

Until recently, nanosecond time-resolved spectroscopy in the far-infrared with high sensitivity has been impossible. When the time-dependent feature is a photoexcitation, pump–probe spectroscopy techniques are attractive. The probe pulse must be suitable for sensing the excitation, and broadband far-infrared pulses have not been available. IR-SR pulses are suitable for such time-resolved spectroscopy.

The far-infrared photoinduced, nanosecond spectroscopy (FIR-PINS) capability that we have developed is a pump–probe technique. The key ingredients are the

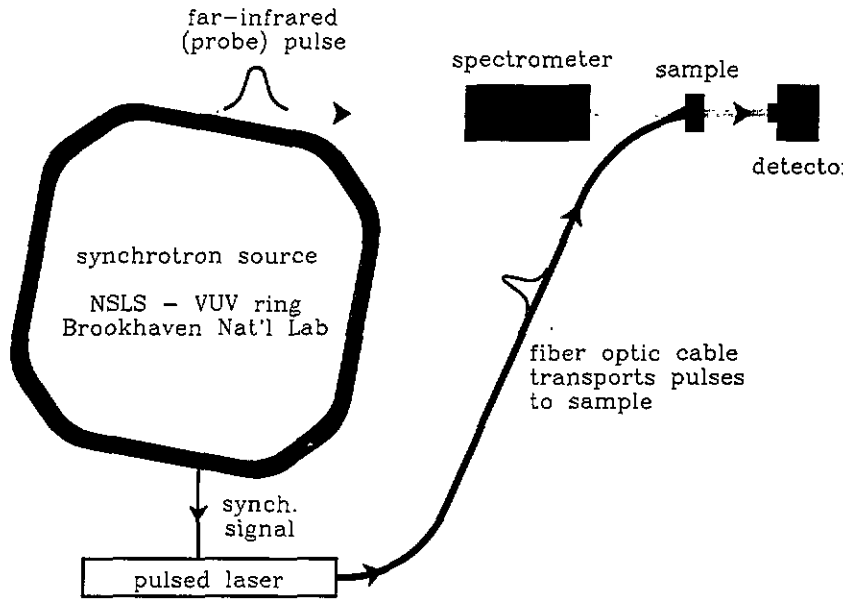

Figure 2. Schematic diagram of the PINS measurement facility.

pulsed photoexcitation (pump) and broadband far-IR (probe) sources. A mode-locked Nd:YAG laser serves as the pump source. The output from a doubling crystal provides 100 ps duration pulses at $\lambda = 0.532\ \mu m$. The mode-locking signal is derived from the synchrotron's RF (52.9 MHz), resulting in pulses that are synchronized to the IR-SR probe pulses. A voltage-controlled phaseshifter is used to adjust the arrival time of the YAG laser pulses relative to the IR-SR pulses. In the present arrangement, an IR-SR pulse arrives once during each RF cycle (~ 19 ns). However, the YAG pulses occur at exactly twice this rate (~ 9.5 ns). This sets an upper limit of about 9 ns to the time range. During a measurement, both the YAG and IR-SR pulses are incident on the sample, with the delay time (between pump and probe pulses) adjusted and recorded. The IR-SR is analysed with a spectrometer just as for a non-time-dependent measurement. A series of measurements with various pump-to-probe delay times are conducted to map out the time-dependent features. A schematic diagram of the technique is shown in figure 2. Other details of the technique are reported elsewhere [9].

We performed PINS measurements on the same MCT sample as described above. The sample was attached to a copper plate with a 1 mm aperture. Both the YAG and IR-SR pulses would pass through this aperture. The plate was clamped to the copper tip of an open-cycle liquid-helium-cooled refrigerator, and placed in the vacuum cell of an IR spectrometer. The detector was a commercial helium-cooled bolometer sensitive only for $\lambda > 100\ \mu m$. A fibre-optic cable was used to bring the YAG pulses to the sample. Transmission measurements were conducted at several temperatures between 10 K and 100 K, and for six different pump-to-probe delay times between 0 ns and 9 ns. At each temperature, a complete set of measurements required about 1 h. This also included a reference spectrum (YAG laser off).

For each pump-to-probe delay time, we calculated the quantity

$$-\Delta T/T \equiv \frac{-(T_{\text{laser on}} - T_{\text{laser off}})}{T_{\text{laser off}}}$$

which is the (negative) differential change in transmission due to exposure by the laser. This is shown in figure 3(*a*) for a YAG pulse fluence of $\sim 3 \times 10^{11}$ photons/cm^2. We note several features, typical of all the measurements, the most prominent being the increasing absorption toward 100 cm^{-1}. This is due to the CdTe substrate's optical phonon near 145 cm^{-1}, which broadens as temperature increases. The 'peaks' near 55 cm^{-1} and 72 cm^{-1} are also thermal in nature, again due to the CdTe substrate. They are far weaker, and probably due to multiphonon absorption processes. Note that both these thermal effects display no time dependence (to within the signal-to-noise, which tends to decrease toward 100 cm^{-1} as the substrate becomes more opaque). The most important feature of the data occurs below 60 cm^{-1}. Here we find the curves separate for the various pump-to-probe delay times, indicating a long-wavelength absorption that decays with time. This is the frequency range where we expect free carrier absorption to be important.

The data can be quantitatively analysed, using standard expressions for the transmission of a thin film on a substrate [10]. The full spectral range can be fitted by including the effects of both phonons and free carriers. In particular, the increasing value of $-\Delta T/T$ toward $\omega = 100$ cm^{-1} can be accurately described using the infrared phonon parameters of Rajavel and Perkowitz [11], assuming a 5 K temperature rise. The free carriers dominate the properties for $\omega < 60$ cm^{-1} and Drude fits yielded values for the scattering time τ and the sheet conductance $\sigma_0 d$ (where d is the film thickness). Only $\sigma_0 d$ displays time dependence. When surface recombination is strong, the photocarrier density is not uniform

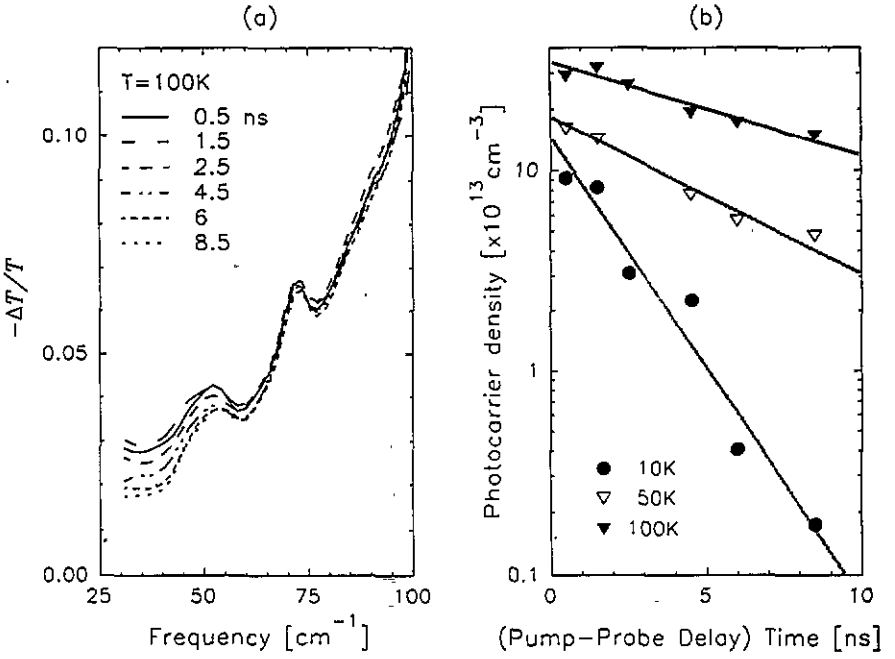

Figure 3. Results from the PINS measurement. (*a*) Change in frequency-dependent transmission (due to the laser pulse) for a range of pump-to-probe delay times. (*b*) Photocarrier density versus time. The full lines are guides to the eye.

throughout the film's depth. However, we can still extract the average, or effective, carrier concentration using $d = 10\ \mu m$ for the film thickness. The results for three temperatures are shown in figure 3(*b*). The photocarrier decay is consistent with a simple exponential, and can be fitted to determine a lifetime.

3. Discussion

Both the wavelength-dependent PCD and the FIR-PINS studies have provided measures of the photocarrier lifetimes. The results are summarized in figure 4, showing the variation with temperature. Agreement between both techniques is very good. The observed lifetimes are short, but not unusual for a non-optimized sample, especially when the surface recombination velocity is high.

We are planning several refinements to enhance the sensitivity and extend the measurement capabilities. For the wavelength-dependent PCD, a wider selection of filters with narrower bandpass is needed for definitive variation and control of the penetration depth. A grating monochromator may be more suitable, especially for tracking the change in bandgap with temperature. Additional amplification should improve the signal-to-noise ratio.

We are also designing improvements to the PINS facility. A system to select only the pulses which match the IR-SR pulses (including single-bunch operation) would reduce the thermal signal and extend the time window to 170 ns. A second possibility is to replace the Nd:YAG laser with a pulsed laser diode system. The diode's lower photon energy would yield a larger photocarrier signal (per watt of power). Also, the present spectrometer is optimized for the 50 cm^{-1} to 700 cm^{-1} (14 μm to 200 μm) range. We expect modifications to improve the long-wavelength performance (where the free carrier absorption is greatest). Another option is to replace the spectrometer with a filter that allows only $\omega < 50\ cm^{-1}$. At such long wavelengths, the transmission change is dominated by the photocarriers.

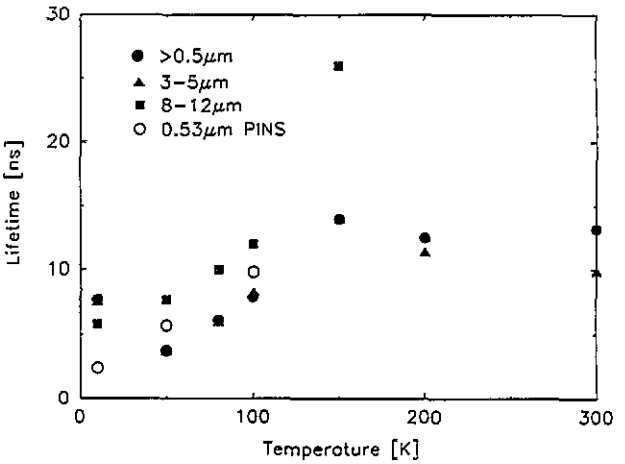

Figure 4. Summary of the photocarrier lifetime for MCT as measured by wavelength-dependent photoconductivity decay (full symbols) and PINS (open circles) as a function of temperature.

We have recently commissioned a separate beamline and spectrometer to cover the $\lambda < 15\ \mu m$ spectral range. At these shorter wavelengths we could investigate the time dependence of the features observed in optical modulation spectroscopy studies [4], which have been attributed to traps or a Burstein-Moss shift [5]. Differences in the time-dependent absorption due to traps could provide new insight into the recombination process when multiple defects are present.

Ideally, we would like to combine the two techniques and use the synchrotron radiation to both generate and sense the photocarriers. This is not easily achieved, due to the requirement that one system should have a large optical delay.

Acknowledgments

Research at Grumman is supported by Independent Research and Development funds. The NSLS is supported by the Department of Energy under contract DE-ACO2-CH00016. We are grateful to A Berghmans (Grumman) for electrical contact preparation, S Etemad (Bellcore) and C J Hirschmugl (NSLS) for assistance with the optical fibre system, D B Tanner (University of Florida) for providing the digitizing oscilloscope, and G P Williams (NSLS) for numerous discussions and advice.

References

[1] Reichman J 1991 *Appl. Phys. Lett.* **59** 1221
[2] See, for example, Baker I M, Capocci F A, Charlton D E and Wotherspoon J T M 1978 *Solid-State Electron.* **21** 1475 and references therein
[3] Spada E J, Rao V R, Bhat I and Borrego J M 1993 *Semicond. Sci. Technol.* **8** 936
[4] Mroczkowski J A, Shanley J F, Reine M B, LoVecchio P and Polla D L 1981 *Appl. Phys. Lett.* **38** 261
Polla D L, Aggarwal R L, Mroczkowski J A, Shanley J F and Reine M B 1982 *Appl. Phys. Lett.* **40** 338
Polla D L, Aggarwal R L, Nelson D A, Shanley J F and Reine M B 1983 *Appl. Phys. Lett.* **43** 941
[5] Doyle O L, Mroczkowski J A and Shanley J F 1985 *J. Vac. Sci. Technol.* A **3** 259
[6] Williams G P 1984 *Int. J. Infrared Millimeter Waves* **5** 829; 1992 *Rev. Sci. Instrum.* **63** 1535
[7] Carr G L, Quijada M, Tanner D B, Hirschmugl C J, Williams G P, Etemad S, Dutta B, DeRosa F, Inam A and Venkatesan T 1990 *Appl. Phys. Lett.* **57** 2725
[8] Scott M W 1969 *J. Appl. Phys.* **40** 4077
Finkman E and Nemirovsky Y 1978 *J. Appl. Phys.* **50** 4356
Mroczkowski J A, Nelson D A, Murosako R and Zimmerman P H 1983 *J. Vac. Sci. Technol.* A **1** 1756
[9] Ederer D L *et al* 1992 *Nucl. Instrum. Methods Phys. Res.* A **319** 250
[10] Gao F *et al* 1991 *Phys. Rev.* B **43** 10383
[11] Rajavel D and Perkowitz S 1988 *J. Electron. Mater.* **17** 25